Slip line analysis of axisymmetric retaining wall interacting with unsaturated soil

Thanh Vo[1], Adrian Russell[1]

[1]Centre for Infrastructure Engineering and Safety, School of Civil and Environmental Engineering, The University of New South Wales, Sydney, NSW, Australia
Corresponding author's E-mail: thanh.vo@unsw.edu.au

Abstract

The slip line theory is applied to the problem of an axisymmetric retaining wall interacting with unsaturated soil. The slip line governing equations express the limiting equilibrium condition of a Mohr-Coulomb soil. A linear variation of the contribution of suction to the effective stress with depth is assumed. Both active and passive failure modes of a rigid wall are considered. The plastic critical depth for unsaturated soil failing in an active failure mode is discussed. Assuming the circumferential stress to be the minor principal stress causes higher passive lateral earth pressure. It is shown that adopting the effective stress concept enables the influence of suction in unsaturated soils to be considered in a simple way. The influence of the contribution of suction to the effective stress is found to be significant.

Keywords: *unsaturated soil, axisymmetric retaining wall, slip line analysis*

1. INTRODUCTION

Retaining walls are used by engineers to resist lateral earth pressure. They often interact with compacted and natural soils above the ground water table. These soils are mostly unsaturated meaning they contain a significant amount of both water and air.

Retaining wall-unsaturated soil interactions have been investigated by some researchers in experiments and theories (Fredlund 1979, Pufahl, Fredlund et al. 1983, Vo 2014, Vo, Taiebat et al. 2016). It has been shown that unsaturated soils are stronger and stiffer than saturated and dry soils. They are also more brittle and prone to shear band formation at a low confining pressure (Vo and Russell 2017).

The slip line theory underpins many design charts in foundation engineering. The effective stress concept for unsaturated soils (Bishop 1959) when combined with the slip line theory has been shown to capture major features of retaining wall-unsaturated soil interactions. Previous slip line analyses of retaining wall-unsaturated soil interaction are limited to a plane strain condition.

Axisymmetric lateral earth pressures are mobilised around a circular excavation and at sites where soil interacts with massive cylindrical structures e.g. circular footing, grain silo, water storage tank, coffer dam, etc. There have been some research applying the slip line theory to axisymmetric retaining walls interacting with dry soils (Cheng, Hu et al. 2007, Liu and Wang 2008, Liu, Wang et al. 2009, Keshavarz and Ebrahimi 2017). The slip line theory has never been applied to axisymmetric retaining walls interacting with unsaturated soils. This paper presents the first slip line analysis of axisymmetric retaining wall interacting with unsaturated soil.

This paper also presents improvements to previous researches on axisymmetric retaining walls interacting with dry soils.

Liu and Wang (2008) analysed an axisymmetric active earth pressure problem but they did not account for the presence of a plastic critical depth that occurs when the total earth pressure at the soil-

wall interface becomes tensile. When this condition develops, soil separates from the rigid wall and changes the boundary conditions. The development of a plastic critical depth has been analysed by some authors for dry soils in a plane strain condition (Peng and Chen 2013, Keshavarz 2016). This paper will consider it for unsaturated soils in axial symmetry.

Keshavarz and Ebrahimi (2017) analysed an axisymmetric passive earth pressure problem by assuming the circumferential stress to be equal to the minor principal stress. This assumption is the Harr-von Karman hypothesis applied to a passive earth pressure problem (Houlsby 1982, Bolton and Lau 1993). This assumption was necessarily adopted for a Tresca soil obeying the associated flow rule (Shield 1952, Houlsby and Wroth 1982) but it is not needed for a Mohr-Coulomb soil. Many authors analysed a Mohr-Coulomb soil in axisymmetric stress-strain regimes where the magnitude of the circumferential stress is neither a major nor minor principal stress (Cox, Eason et al. 1961, Drescher 1986, Hill and Cox 2000).

The Harr-von Karman hypothesis for an active earth pressure problem states that the circumferential stress is equal to the major principal stress. Much experimental and numerical evidence shows that adopting this hypothesis is not conservative for a Mohr-Coulomb soil in an active failure mode (Cheng, Au et al. 2008, Tobar and Meguid 2011, Kim, Lee et al. 2013, Cho, Hyunsung et al. 2015), since it underestimates the lateral earth pressure at failure.

There is no direct measurement of the magnitude of the circumferential stress for a Mohr-Coulomb soil (Keshavarz and Ebrahimi 2017). Experimental evidence for the Harr-von Karman hypothesis in a passive failure mode has never been presented. Hill (1950) considered this hypothesis to be overly restrictive. Hansen, Christensen et al. (1968) expressed reservations about the hypothesis being applied to the axisymmetric bearing capacity problem on a Mohr-Coulomb soil.

In this paper, the authors present analyses to show that the Harr-von Karman hypothesis is not conservative in a passive failure mode. It is shown that adopting the Harr-von Karman hypothesis in a passive failure mode results in higher lateral earth pressure than without adopting it.

2. GOVERNING EQUATIONS

2.1. Effective stress and failure criterion

It is assumed that soil shear strength is governed by the Mohr-Coulomb failure criterion:

$$\tau = c' + \sigma'_{\mathrm{m}} \tan \varphi' \tag{1}$$

in which c' is the soil cohesion and φ' is the soil friction angle obtained from axisymmetric soil tests e.g. triaxial test. σ'_{m} is mean effective stress and for an unsaturated soil is defined as (Bishop 1959):

$$\sigma'_{\mathrm{m}} = \sigma_{\mathrm{m}} - u_{\mathrm{a}} + \chi(u_{\mathrm{a}} - u_{\mathrm{w}}) \tag{2}$$

where σ_{m} is mean total stress, u_{a} is pore air pressure, u_{w} is pore water pressure and χ is effective stress parameter. When pore air pressure is equal to atmospheric pressure and is taken as the pressure datum, Eq. 2 can be written as:

$$\sigma'_{\mathrm{m}} = \sigma_{\mathrm{m}} + \chi s \tag{3}$$

where $s = u_{\mathrm{a}} - u_{\mathrm{w}}$ is soil suction. χs is the contribution of suction to the effective stress. It is assumed that φ' is constant in this paper.

2.2. Cohesion and contribution of suction to the effective stress

Unsaturated frictional soils are treated as non-homogeneous soils in this paper. The non-homogeneity may occur in the soil cohesion (c') and the contribution of suction to the effective stress (χs). For simplicity, it is assumed that c' is constant and χs varies linearly with depth by the functions:

$$\chi s = (\chi s)_0 + k_{\chi s} z \tag{4}$$

where $(\chi s)_0$ is contribution of suction to the effective stress at $z = 0$ and $k_{\chi s}$ is a constant. Non-homogeneity in the soil cohesion has been treated by several authors (Davis and Booker 1973, Tani and Craig 1995, Hu and Randolph 1998). This paper focuses on the non-homogeneity occurring in the contribution of suction to the effective stress.

2.3. Governing equations of the stress slip lines

With reference to the coordinates system shown in Fig. 1, the static equilibrium equations are expressed as:

$$\frac{\partial \sigma_{rr}}{\partial r} + \frac{\partial \sigma_{rz}}{\partial z} + \frac{\sigma_{rr} - \sigma_{\theta\theta}}{r} = 0 \tag{5}$$

$$\frac{\partial \sigma_{rz}}{\partial r} + \frac{\partial \sigma_{zz}}{\partial z} + \frac{\sigma_{rz}}{r} = \gamma_t \tag{6}$$

where σ_{zz}, σ_{rr} are normal stresses in the z and r directions, respectively, $\sigma_{\theta\theta}$ is circumferential stress, σ_{zr} is shear stress and γ_t is soil unit weight. At the onset of failure, the stress components $\sigma_{zz}, \sigma_{rr}, \sigma_{zr}$ satisfy:

$$\sigma_{zz} = [(1 + \sin\varphi' \cos 2\psi)\sigma'_m - c' \cot\varphi'] - \chi s \tag{7}$$

$$\sigma_{rr} = [(1 - \sin\varphi' \cos 2\psi)\sigma'_m - c' \cot\varphi'] - \chi s \tag{8}$$

$$\sigma_{zr} = \sigma'_m \sin\varphi' \sin 2\psi \tag{9}$$

where ψ is angle between the vertical axis and the major principal stress direction. The circumferential stress $\sigma_{\theta\theta}$ is assumed to be intermediate between the major and minor principal stresses:

$$\sigma_{\theta\theta} = k_{\theta\theta}[(1 \pm \sin\varphi')\sigma'_m - c' \cot\varphi'] - \chi s \tag{10}$$

where $k_{\theta\theta}$ is a constant, the (+) sign in Eq. 10 applies to an active failure mode and the (-) sign in Eq. 10 applies to a passive failure mode. In this paper, the constant $k_{\theta\theta}$ will be varied to investigate the influence of the magnitude of the circumferential stress. $k_{\theta\theta}$ is restricted theoretically as $\frac{(1-\sin\varphi')\sigma'_m - c'\cot\varphi'}{(1+\sin\varphi')\sigma'_m - c'\cot\varphi'} \le k_{\theta\theta} \le 1$ in an active failure mode and $1 \le k_{\theta\theta} \le \frac{(1+\sin\varphi')\sigma'_m - c'\cot\varphi'}{(1-\sin\varphi')\sigma'_m - c'\cot\varphi'}$. The magnitude of $k_{\theta\theta}$ will be discussed later in section 4.2.

The stress components (Eqs. 7-10) are substituted into Eqs. 5-6 and solved to obtain two families of stress slip lines (ξ, η):

$$\langle \xi \rangle \equiv \begin{cases} \mathrm{d}r = \tan(\psi - \mu)\mathrm{d}z \\ -\mathrm{d}\sigma'_m + 2\tan\varphi' \sigma'_m \mathrm{d}\psi = A\left[-\frac{\sin(\psi+\mu)}{\cos^2\varphi'}\mathrm{d}z + \frac{\cos(\psi+\mu)}{\cos^2\varphi'}\mathrm{d}r\right] \end{cases} \tag{11}$$

$$\langle \eta \rangle \equiv \begin{cases} \mathrm{d}r = \tan(\psi + \mu)\mathrm{d}z \\ \mathrm{d}\sigma'_m + 2\tan\varphi' \sigma'_m \mathrm{d}\psi = B\left[\frac{\sin(\psi-\mu)}{\cos^2\varphi'}\mathrm{d}z - \frac{\cos(\psi-\mu)}{\cos^2\varphi'}\mathrm{d}r\right] \end{cases} \tag{12}$$

where

$$A = \sin(\psi + \mu)\left[\gamma_t + \frac{\partial(\chi s)}{\partial z} - \frac{\sigma'_m \sin\varphi' \sin 2\psi}{r}\right] + \cos(\psi + \mu)\left[\frac{\sigma'_m(1-\sin\varphi'\cos 2\psi) - c'\cot\varphi'(1-k_{\theta\theta}) - (1\pm\sin\varphi')\sigma'_m k_{\theta\theta}}{r}\right] \tag{13}$$

and

$$B = \sin(\psi - \mu)\left[\gamma_t + \frac{\partial(\chi s)}{\partial z} - \frac{\sigma'_m \sin\varphi' \sin 2\psi}{r}\right] + \cos(\psi - \mu)\left[\frac{\sigma'_m(1-\sin\varphi'\cos 2\psi) - c'\cot\varphi'(1-k_{\theta\theta}) - (1\pm\sin\varphi')\sigma'_m k_{\theta\theta}}{r}\right] \quad (14)$$

and $\mu = \frac{\pi}{4} - \frac{\varphi'}{2}$.

3. THE AXISYMMETRIC RETAINING WALL PROBLEM

3.1. Problem definition

A typical axisymmetric retaining wall interacting with unsaturated frictional soil is shown in Fig. 1. The wall OA is at a distance r_0 from the axis of symmetry. An active and a passive failure mode corresponds to the soil below OB reaching a minimal and a maximal stress state, respectively (Sokolovski 1954). The soil-wall interface friction angle is negative in an active failure and positive in a passive failure mode. The wall OA is inclined at angle α from the vertical (α is negative clockwise and positive anticlockwise).

Eqs. 11-14 show that as $r_0 \to \infty$, the axisymmetric retaining wall problem becomes the corresponding plane strain problem (Vo and Russell 2017). Eqs. 11-14 also show that design charts for the axisymmetric retaining wall problem must contain r_0 (Liu and Wang 2008, Keshavarz and Ebrahimi 2017).

3.2. Boundary conditions

Boundary conditions of this problem include the soil surface OB, point O and the retaining wall-soil interface OA (Fig. 1). At the soil surface OB, $\psi = 0, \sigma'_m = \frac{q + c'\cot\varphi' + (\chi s)_0}{1+\sin\varphi'}, z = 0, r = r_0 + [0, \overline{OB}]$ in an active failure mode and $\psi = \frac{\pi}{2}, \sigma'_m = \frac{q + c'\cot\varphi' + (\chi s)_0}{1-\sin\varphi'}, z = 0, r = r_0 + [0, \overline{OB}]$ in a passive failure mode where q is the surcharge applied on OB. At the soil-wall interface OA, $\psi = \left(\frac{\Delta'}{2} - \frac{\delta'}{2}\right) + \alpha, \frac{z}{r_0 - r} = \tan\left(\frac{\pi}{2} - \alpha\right)$ in an active failure mode and $\psi = \frac{\pi}{2} - \left(\frac{\Delta'}{2} + \frac{\delta'}{2}\right) - \alpha, \frac{z}{r_0 - r} = \tan\left(\frac{\pi}{2} - \alpha\right)$ in a passive failure mode where Δ' is defined by $\Delta' = \sin^{-1}\left(\frac{\sin\delta'}{\sin\varphi'}\right)$ and α is the wall inclination angle. Point O is treated as a slip line in the limit so ψ, σ' transit from their values on OB to their values on OA.

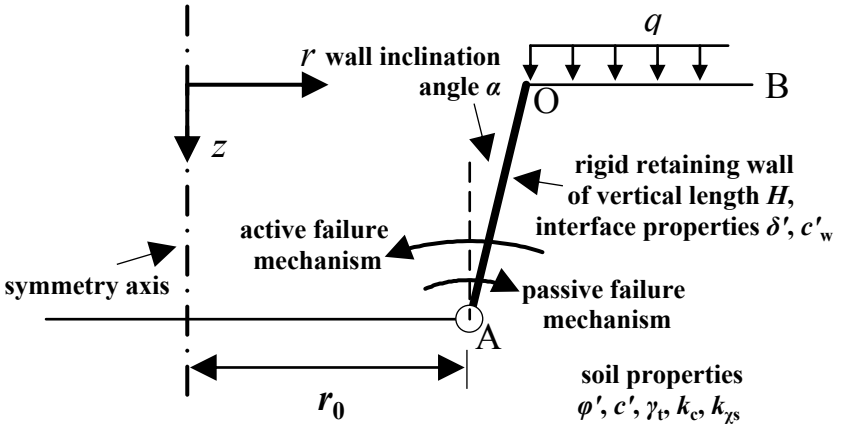

Figure 1. Coordinates system and problem geometry.

3.3. Solution procedures

The governing equations and boundary conditions were solved using a finite difference procedure similar to Sokolovski (1954). The numerical procedures were verified by reproducing the results of Liu and Wang (2008) (an active failure mode) and Keshavarz and Ebrahimi (2017) (a passive failure mode). Using only 100 characteristic pairs, exact agreements are achieved as shown in Figs. 2. In Fig. 2a, when the total normal stress on rigid retaining wall becomes tensile, the soil separates from the rigid wall and changes the boundary conditions. This issue will be investigated in the next section. In Fig. 2b, c'_{w} denotes the cohesion coefficient at the soil-wall interface.

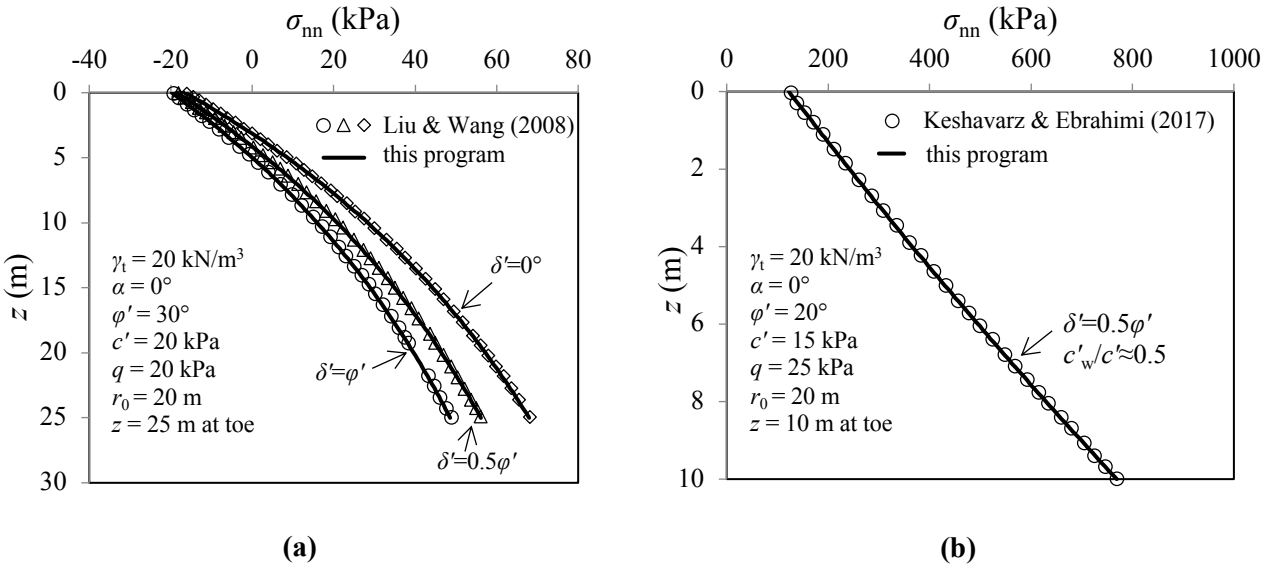

Figure 2. Validation against the results of (a) Liu and Wang (2008) for an active failure mode and (b) Keshavarz and Ebrahimi (2017) for a passive failure mode.

4. RESULTS

4.1. Plastic critical depth in an active failure mode

When $(\sigma_{\mathrm{nn}})_{\mathrm{O\_rw}} < 0$, soil separates from the rigid wall and changes the boundary conditions. The greatest depth where this occurs is denoted z_{cr} and can be referred to as the plastic critical depth. In this paper, the following assumptions are made:

- It is assumed that above the plastic critical depth, the soil is in an elastic state. The new surface boundary is $O_{cr}B_{cr}$ (Fig. 3). The new surcharge will be $q_{\mathrm{cr}} = \gamma_{\mathrm{t}} z_{\mathrm{cr}} + q$ where $\gamma_{\mathrm{t}} z_{\mathrm{cr}}$ represents the weight of the elastic soil. For simplicity, this new surcharge is assumed to be uniformly distributed on $O_{cr}B_{cr}$. This approximation is most correct when the retaining wall is near vertical (i.e. α is small).
- It is assumed that above the plastic critical depth, the contribution of suction to the effective stress is constant at $\chi s = (\chi s)_0$ and below the plastic critical depth $\chi s = (\chi s)_0 + k_{\chi s}(z - z_{\mathrm{cr}})$.

The plastic critical depth z_{cr} can be found by computing the total normal stress on the wall at point O and setting it to zero. How to do this is described below.

The effective mean stress on the retaining wall at point O is denoted $(\sigma'_{\mathrm{m}})_{\mathrm{O\_rw}}$ and is found to be:

$$(\sigma'_{\mathrm{m}})_{\mathrm{O\_rw}} = \left[\frac{q + c' \cot\varphi' + (\chi s)_0}{1 + \sin\varphi'}\right] e^{2\tan\varphi'\left(\frac{\Delta'}{2} - \frac{\delta'}{2} + \alpha\right)} \tag{15}$$

The total normal stress on the retaining wall at point O is denoted $(\sigma_{nn})_{O\_rw}$ and is found to be:

$$(\sigma_{nn})_{O_{rw}} = [1 - \sin\varphi' \cos(\Delta' - \delta')]\left[\frac{q + c' \cot\varphi' + (\chi s)_0}{1 + \sin\varphi'}\right] e^{2\tan\varphi'\left(\frac{\Delta'}{2} - \frac{\delta'}{2} + \alpha\right)} - c' \cot\varphi' - (\chi s)_0 \quad (16)$$

Requiring $(\sigma_{nn})_{O\_rw} = 0$ results in:

$$q_{cr} = [c' \cot\varphi' + (\chi s)_0]\left[\frac{(1+\sin\varphi') e^{-2\tan\varphi'\left(\frac{\Delta'}{2} - \frac{\delta'}{2} + \alpha\right)}}{1 - \sin\varphi' \cos(\Delta' - \delta')} - 1\right] \quad (17)$$

In Eq. 17, q_{cr} is the minimum surcharge for $(\sigma_{nn})_{O\_rw} \geq 0$. Consequently, z_{cr} is found to be:

$$z_{cr} = \frac{[c' \cot\varphi' + (\chi s)_0]\left[\frac{(1+\sin\varphi') e^{-2\tan\varphi'\left(\frac{\Delta'}{2} - \frac{\delta'}{2} + \alpha\right)}}{1 - \sin\varphi' \cos(\Delta' - \delta')} - 1\right] - q}{\gamma_t} \quad (18)$$

Eq. 18 implies higher surcharge, higher $c' \cot\varphi'$, or higher $(\chi s)_0$will result in higher plastic critical depth z_{cr}.

Table 1 lists parameters of analyses 1-2. Parameters of analysis 1 are based on Liu and Wang (2008). Analysis 1 was also used in the numerical verification process (section 3.3, Fig. 2a). The results of analyses 1-2 are plotted in Fig. 4.

It is shown that the existence of tensile total normal stress at the soil-wall interface in analysis 1 has been eliminated by adopting $q_{cr} = 69.28, 83.02, 92.18$ kPa in analysis 2 (calculated using Eq. 17). Assuming the original surcharge $q = 20$ kPa in analysis 1 is still being applied, the net surcharges (i.e. the weight of the elastic soil) in analysis 2 are $q_{cr} - q = 46.28, 63.02, 72.18$ kPa. The plastic critical depths corresponding to these surcharges are $z_{cr} = 2.464, 3.151, 3.609$ m, respectively.

Fig. 4 shows that when the plastic critical depths are accounted for, the total normal earth pressures on the retaining wall are always compressive. Fig. 4 also shows that below the plastic critical depths, the total normal earth pressures increase slightly.

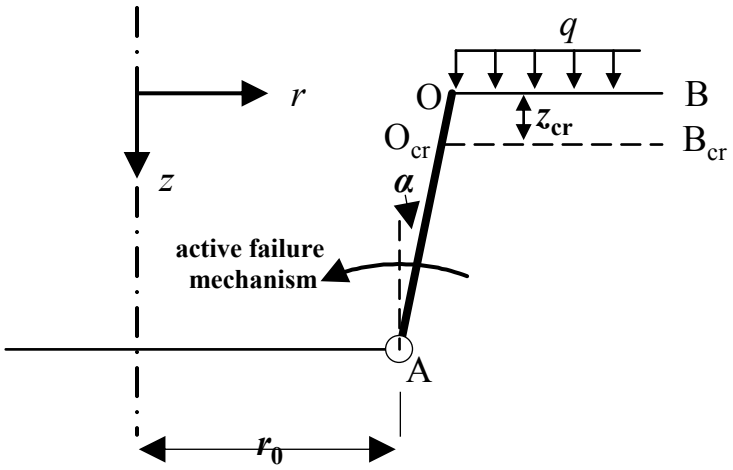

Figure 3. Occurrence of plastic critical depth (z_{cr}) in an active failure mode.

Table 1. Parameters adopted in analyses 1-7.

parameters	unit	analysis 1	analysis 2	analysis 3	analysis 4	analysis 5	analysis 6 (active mode)	analysis 7 (passive mode)
φ'	°	30	30	20	20	25	25	25
δ'	°	0,15,30	0,15,30	10	10	12.5	12.5	12.5
c'	kPa	20	20	15	15	17.5	17.5	17.5
$(\chi s)_0$	kPa	0	0	0	0	0	20,40	20,40
$k_{\chi s}$	kPa/m	0	0	0	0	0	-1	-1
q	kPa	20	20	25	25	22.5	22.5	22.5
q_{cr}	kPa	N/A	69.28,83.02,92.18	N/A	N/A	N/A	N/A	N/A
γ_{t}	kN/m^3	20	20	20	20	20	20	20
α	°	0	0	0	0	0	0	0
r_0	m	20	20	20	20	20	20	20
$k_{\theta\theta}$	n. a.	1	1	1	1.922,3.845	1	1	1
H	m	25	25	10	10	17.5	17.5	17.5

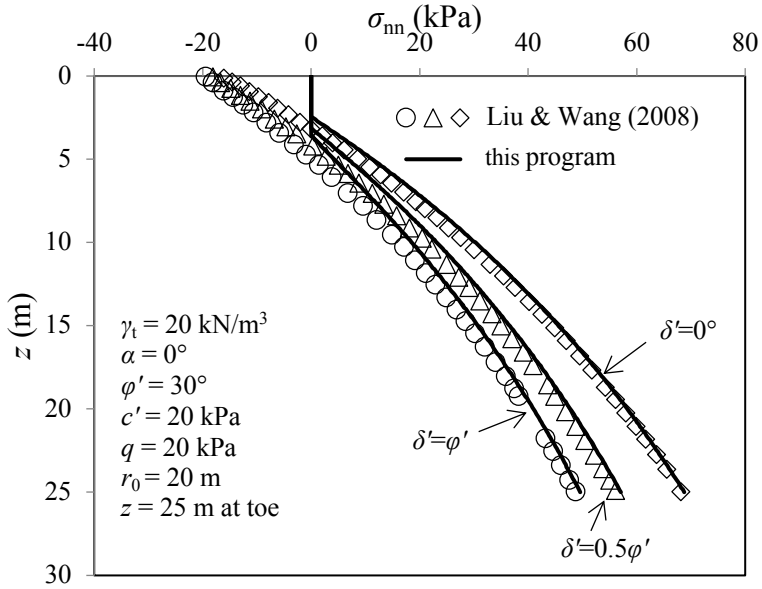

Figure 4. Lateral earth pressures on a retaining wall in an active failure mode when plastic critical depths are accounted for.

4.2. Influence of the relative magnitude of the circumferential stress in a passive failure mode

The limiting equilibrium equations (Eqs. 5-10) are determinate if $k_{\theta\theta}$ is known. The Harr-von Karman hypothesis (Harr and von Kármán 1909) applied for a passive earth pressure problem states that the circumferential stress is equal to the minor principal stress. This assumption was adopted previously to calculate the bearing capacity of a circular footing and the penetration resistance of a conical indenter. More recently, it is used to calculate the passive lateral earth pressure on an axisymmetric retaining wall (Keshavarz and Ebrahimi 2017).

In a passive failure mode, the soil is displaced outwards by the wall, thus inducing a tensile circumferential strain (Houlsby and Wroth 1982). As most soils have little shear strength when in tension, the circumferential stress should be closer to the minor principal stress than the major principal stress.

There is no direct measurement of the magnitude of the circumferential principal stress (Keshavarz and Ebrahimi 2017). Many researchers assumed that it is equal to the minor principal stress for a Mohr-Coulomb soil (Bolton and Lau 1993, Cassidy and Houlsby 2002, Martin 2004). Some researchers constrained it to be closer to the minor principal stress than the major principal stress (Kumar and Khatri 2011, Chakraborty and Kumar 2014, Bhattacharya and Kumar 2016).

Table 1 lists parameters of analyses 3-4. Parameters of analysis 3 are based on Keshavarz and Ebrahimi (2017). Analysis 4 is different from analysis 3 in the relative magnitude of the circumferential stress. In analysis 3, $k_{\theta\theta} = 1$ compared to in analysis 4, $k_{\theta\theta} = 1.922, 3.845$. It is noted that $k_{\theta\theta} = 1$ corresponds to the assumption that the circumferential stress is equal to the minor principal stress whereas $k_{\theta\theta} = 3.845 = \frac{1+\sin 20^\circ}{1-\sin 20^\circ}$ is an upper bound of $k_{\theta\theta}$, obtained when $c' = 0$ kPa. The $k_{\theta\theta}$ values adopted in analysis 4 were deliberately high (although they are theoretically permissible) to demonstrate the impact of Harr-von Karman hypothesis. The results of analyses 3-4 are plotted in Fig. 5.

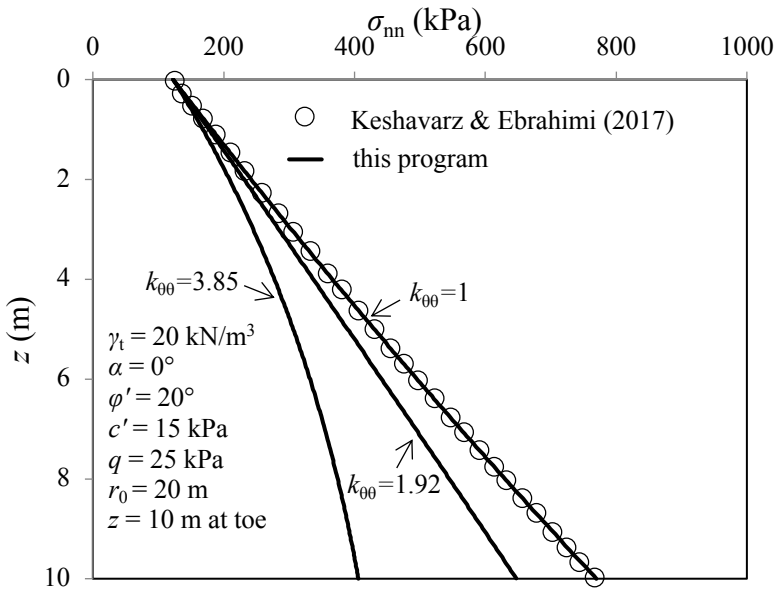

Figure 5. Influence of the magnitude of the circumferential stress in a passive failure mode.

Fig. 5 shows that assuming the circumferential stress equal to the minor principal stress i.e. $k_{\theta\theta} = 1$ results in significantly higher lateral earth pressure on retaining wall. This means that given certain soil strength parameters, a higher passive thrust is needed to cause failure. Clearly, the $k_{\theta\theta} = 1$ assumption leads to non-conservative results.

4.3.Influence of the contribution of suction to the effective stress

Table 1 lists parameters of analyses 5-7. The results of analyses 5-7 are plotted in Figs. 6. In analysis 5, $(\chi s)_0 = 0$ kPa, $k_{\chi s} = 0$ kPa/m to simulate a dry condition while in analyses 6-7, $(\chi s)_0 = 20{,}40$ kPa, $k_{\chi s} = -1$ kPa/m to simulate unsaturated conditions. Analysis 6 assumes an active failure mode and analysis 7 assumes a passive failure mode.

Figs. 6 show that the impacts of the contribution of suction to effective stress are significant in both active and passive failure modes. Suction in unsaturated soil increases the effective normal pressures at the soil-wall interface. The occurrence of plastic critical depths in an active failure mode causes very different lateral earth pressure profiles to be mobilised at limiting condition (Fig. 6a).

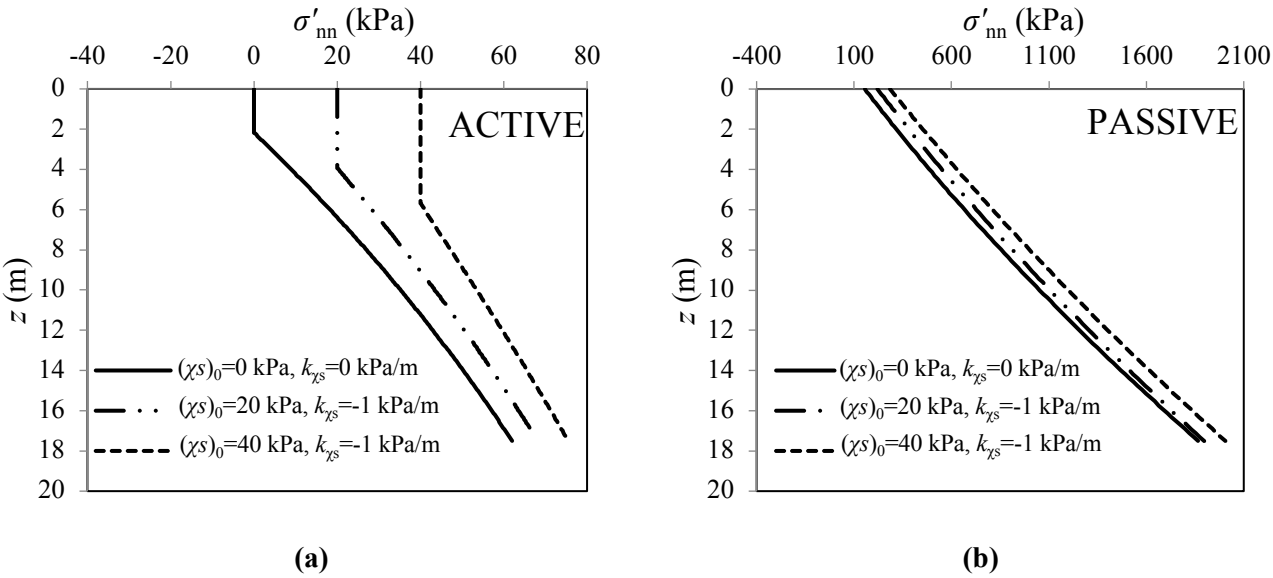

Figure 6. Influence of the contribution of suction to the effective stress on the distribution of effective lateral earth pressure on retaining wall for (a) an active failure mode and (b) a passive failure mode.

5. CONCLUSION

The slip line theory has been applied to an axisymmetric retaining wall-unsaturated soil interaction problem. Assuming the wall reaching an active failure mode and a passive failure mode, the governing equations are presented and solved iteratively using the finite difference method. An expression is presented for estimating the plastic critical depth in an active failure mode in unsaturated soils. It is also shown that assuming the circumferential stress to be equal to the minor principal stress in a passive failure mode is not conservative. It is shown that adopting the effective stress concept enables the influence of suction in unsaturated soils to be considered in a simple way. The influence of the contribution of suction to the effective stress is found to be significant.

REFERENCES

Bhattacharya, P. and J. Kumar (2016). "Uplift capacity of anchors in layered sand using finite element limit analysis: formulation and results." International Journal of Geomechanics **16**(3).

Bishop, A. W. (1959). "The principle of effective stress." Teknisk Ukeblad **106**(39): 859-863.

Bolton, M. D. and C. K. Lau (1993). "Vertical bearing capacity factors on mohr coulomb soil." Canadian Geotechnical Journal **30**(6): 1024-1033.

Cassidy, M. J. and G. T. Houlsby (2002). "Vertical bearing capacity factors for conical footings on sand." Géotechnique **52**(9): 687-692.

Chakraborty, M. and J. Kumar (2014). "Bearing capacity of circular foundations reinforced with geogrid sheets." Soils and Foundations **54**(4): 820-832.

Cheng, Y. M., et al. (2008). "Active pressure for circular cut with Berezantzev's and Prater's theories, numerical modeling and field measurements." Soils and Foundations **48**(5): 621-631.

Cheng, Y. M., et al. (2007). "General axisymmetric active earth pressure by method of characteristics: theory and numerical formulation." International Journal of Geomechanics **7**(1): 1-15.

Cho, J., et al. (2015). "Analysis of lateral earth pressure on a vertical circular shaft considering the 3D arching effect." Tunnelling and Underground Space Technology **48**(April): 11-19.

Cox, A. D., et al. (1961). "Axially symmetric plastic deformations in soils." Philosophical Transactions of the Royal Society of London. Series A, Mathematical and Physical Sciences **254**(1036): 1-45.

Davis, E. H. and J. R. Booker (1973). "The effect of increasing strength with depth on the bearing capacity of clays." Géotechnique **23**(4): 551-563.

Drescher, A. (1986). "Kinematics of axisymmetric vertical slopes at collapse." International Journal for Numerical and Analytical Methods in Engineering **10**(4): 431-441.

Fredlund, D. (1979). "Second Canadian geotechnical colloquium appropriate concepts and technology for unsaturated soils." Canadian Geotechnical Journal **16**(1): 121-139.

Hansen, B., et al. (1968). "Discussion of "Theoretical bearing capacity of very shallow footings"." Journal of Soil Mechanics and Foundations Division ASCE **95**(SM9): 1568-1573.

Harr, A. and T. von Kármán (1909). "Zur Theorie der Spannungszustäende in Plastischen und Sandartigen Medien. Nachrichten Von der Königlichen Gesellschaft der Wissenschaften zu Göttingen." Math. Phys. Klasse.

Hill, J. M. and G. M. Cox (2000). "Cylindrical cavities and classical rat-hole theory occuring in bulk materials." International Journal for Numerical and Analytical Methods in Geomechanics **24**(12): 971-990.

Hill, R. (1950). The Mathematical Theory of Plasticity, Oxford University Press.

Houlsby, G. (1982). "Theoretical analysis of fall cone test." Géotechnique **32**(2): 111-118.

Houlsby, G. T. and C. P. Wroth (1982). Determination of undrained strengths by cone penetration tests. Proceedings of the 2nd European Symposium on Penetration Testing, Amsterdam.

Hu, Y. and M. F. Randolph (1998). "Deep penetration of shallow foundations on non-homogeneous soil." Soils and Foundations **38**(1): 241-246.

Keshavarz, A. (2016). "Evaluation of the palstic critical depth in seismic active lateral earth pressure problems using the stress characteristics method." Acta Geotechnica Slovenica **13**(2016/1): 17-25.

Keshavarz, A. and M. Ebrahimi (2017). "Axisymmetric passive lateral earth pressure of retaining walls." KSCE Journal of Civil Engineering **21**(5): 1706-1716.

Kim, K. K., et al. (2013). "The effect of arching pressure on a vertical circular shaft." Tunnelling and Underground Space Technology **37**: 10-21.

Kumar, J. and V. N. Khatri (2011). "Bearing capacity fators for circular foundations for a general c-phi soil using lower bound finite elements limit analysis." International Journal for Numerical and Analytical Methods in Geomechanics **35**: 393-405.

Liu, F. and J. Wang (2008). "A generalized slip line solution to the active earth pressure on circular retaining walls." Computers and Geotechnics **35**(2): 155-164.

Liu, F. Q., et al. (2009). "Axi-symmetric active earth pressure obtained by the slip line method with a general tangential stress coefficient." Computers and Geotechnics **36**(1-2): 352-358.

Martin, C. M. (2004). User guide for ABC - analysis of bearing capacity version 1.0. UK, University of Oxford.

Peng, M. X. and J. Chen (2013). "Slip line solution to active earth pressure on retaining walls." Géotechnique **63**(12): 1008-1019.

Pufahl, D. E., et al. (1983). "Lateral earth pressure in expansive clay soils." Canadian Geotechnical Journal **20**(2): 228-241.

Shield, R. T. (1952). Stress and velocity fields in soil mechanics, Brown University.

Sokolovski, W. V. (1954). Statics of Soil Media. London, UK, Butterworths.

Tani, K. and W. H. Craig (1995). "Bearing capacity of circular foundations on soft clay of strength increasing with depth." Soils and Foundations **35**(4): 21-35.

Tobar, T. and M. A. Meguid (2011). "Experimental study of the earth pressure distribution on cylindrical shafts." Journal of Geotechnical and Geoenvironmental Engineering **137**(11): 1121-1125.

Vo, T. (2014). Interaction between a rigid retaining wall and unsaturated soils. School of Civil and Environmental Engineering. Sydney, UNSW. **PhD**.

Vo, T. and A. R. Russell (2017). "Interaction between retaining walls and unsaturated soils in experiments and using slip line theory." Journal of Engineering Mechanics **143**(4).

Vo, T. and A. R. Russell (2017). "Stability charts for curvilinear slopes in unsaturated soils." Soils and Foundations **57**(4): 543-556.

Vo, T., et al. (2016). "Interaction of a rotating rigid retaining wall with unsaturated soil in experiments." Géotechnique **66**(5): 366-377.